Boletim da Sociedade Astronômica Brasileira, **35**, no. 1, 258-262

Cosmic rays acceleration by magnetic reconnection in relativistic jets by means of in situ 3D MHD-PIC simulations

T. E. Medina-Torrejón[1], E. M. de Gouveia Dal Pino[2], e G. Kowal[3]

[1] Instituto de Física de São Carlos, Universidade de São paulo, São Paulo
e-mail: temt@usp.br
[2] Instituto de Astronomia, Geofísica e Ciências Atmosféricas, São Paulo University, São Paulo
e-mail: dalpino@iag.usp.br
[3] Escola de Artes, Ciências e Humanidades, São Paulo University, São Paulo
e-mail: grzegorz.kowal@usp.br

Abstract. The origin of the cosmic rays is still an open question. Observations have shown that magnetically dominated environments (such as the sources of surrounding black holes and the base of relativistic jets from AGNs, microquasars, and GRBs) produce very high-energy emissions (VHE). This VHE emission is especially present in blazars, with time-variability from days to minutes (in the GeV and TeV bands), which implies very compact emission regions. The most probable mechanism able to explain this high variability and compactness of the TeV emission seems to be fast magnetic reconnection. Our earlier works based on 3D MHD simulations of relativistic jets, have evidenced, for the first time, that particle acceleration by magnetic reconnection driven by the turbulence in the flow of relativistic jets occurs from the resistive up to the large injection scale of the turbulence. Particles are exponentially accelerated in time by magnetic reconnection in a stochastic Fermi process up to ultra-high-energies. In this work, we will show the results of MHD-particle-in-cell (MHD-PIC) simulations following the early stages of the particle acceleration evolving with the relativistic jet, which confirm our previous results, demonstrating the strong potential of magnetic reconnection driven by turbulence to accelerate relativistic particles to extreme energies in magnetically dominated flows.

Resumo. A origem dos raios cósmicos ainda é uma questão em aberto. As observações mostram que ambientes dominados magneticamente (como fontes de buracos negros e a base de jatos relativísticos de AGNs, microquasares e GRBs) produzem emissões de energia muito alta (VHE das sigas em ingles). Esta emissão de VHE está especialmente presente em blazares, com variabilidade temporal de dias a minutos (nas bandas GeV e TeV), o que implica regiões de emissão muito compactas. O mecanismo mais provável capaz de explicar esta alta variabilidade e compacidade da emissão de TeV parece ser a reconexão magnética rápida. Nossos trabalhos anteriores baseados em simulações 3D MHD de jatos relativísticos evidenciaram, pela primeira vez, que a aceleração de partículas por reconexão magnética impulsionada pela turbulência no fluxo de jatos relativísticos ocorre desde o limite resistivo até as grandes escalas de injeção da turbulência. As partículas são aceleradas exponencialmente no tempo por reconexão magnética em um processo de Fermi estocástico até energias ultra-altas. Neste trabalho, mostraremos os resultados de simulações MHD-particle-in-cell (MHD-PIC) seguindo os estágios iniciais da aceleração das partículas evoluindo com o jato relativístico, que confirmam nossos resultados anteriores, demonstrando o forte potencial de reconexão magnética impulsionado pela turbulência para acelerar partículas relativísticas a energias extremas em fluxos dominados magneticamente.

Palavras-chave. acceleration of particles – magnetic reconnection – instabilities – magnetohydrodynamics (MHD) – methods: numerical

1. Introdução

Blazars (relativistic jets pointing to the line-of-sight) produce usually highly variable, non-thermal emission in all wavelengths, which is generally attributed to relativistic particles (protons and electrons) accelerated stochastically in recollimation shocks along the jet and in their head (Mizuno et al. 2015; Hovatta and Lindfors 2019; Matthews et al. 2020, e.g.). However, there is increasing evidence that shock acceleration may not be always as efficient in the magnetically dominated regions of these jets, particularly to explain the very high energy (VHE) emission (Sironi et al. 2013; de Gouveia Dal Pino and Kowal 2015; Bell et al. 2018). The truth is that, under these conditions, the acceleration mechanisms of these particles at VHE are still unknown.

The magnetic reconnection is a strong candidate for the production of ultra-high energy cosmic rays (UHECRs) and VHE flares in the magnetically dominated regions of relativistic sources (e.g., Cerutti et al. 2013; Christie et al. 2019; Mehlhaff et al. 2020; Kadowaki et al. 2021; Medina-Torrejón et al. 2021, 2023; Zhang et al. 2023), and for these reason it has lately gained tremendous importance in high energy astrophysics (de Gouveia Dal Pino and Lazarian 2005; Giannios et al. 2009; de Gouveia Dal Pino et al. 2010; Zhang and Yan 2011; Hoshino and Lyubarsky 2012; McKinney and Uzdensky 2012; Kadowaki et al. 2015; Zhang et al. 2018).

The comprehension of particle acceleration driven by magnetic reconnection has greatly improved thanks to both particle-in-cell (PIC) simulations (predominantly performed in two-dimensions - 2D) (e.g., Zenitani and Hoshino 2001; Drake et al. 2006; Zenitani and Hoshino 2007; Sironi and Spitkovsky 2014; Guo et al. 2015, 2020; Sironi et al. 2015; Ball et al. 2018; Kilian et al. 2020; Sironi 2022)), and MHD simulations (generally performed in 3D) (e.g., Kowal et al. 2011, 2012; del Valle et al. 2016; Beresnyak and Li 2016; Guo et al. 2019; Medina-Torrejón et al. 2021, 2023). They both have established reconnection as an efficient process of acceleration.

More recently MHD studies, Medina-Torrejón et al. (2021, hereafter MGK+21) and Kadowaki et al. (2021, hereafter KGM+21), motivated by current debates related to the origin of cosmic ray acceleration and VHE variable emission in relativistic jets, and specially in blazars (e.g., Aharonian et al. 2007;

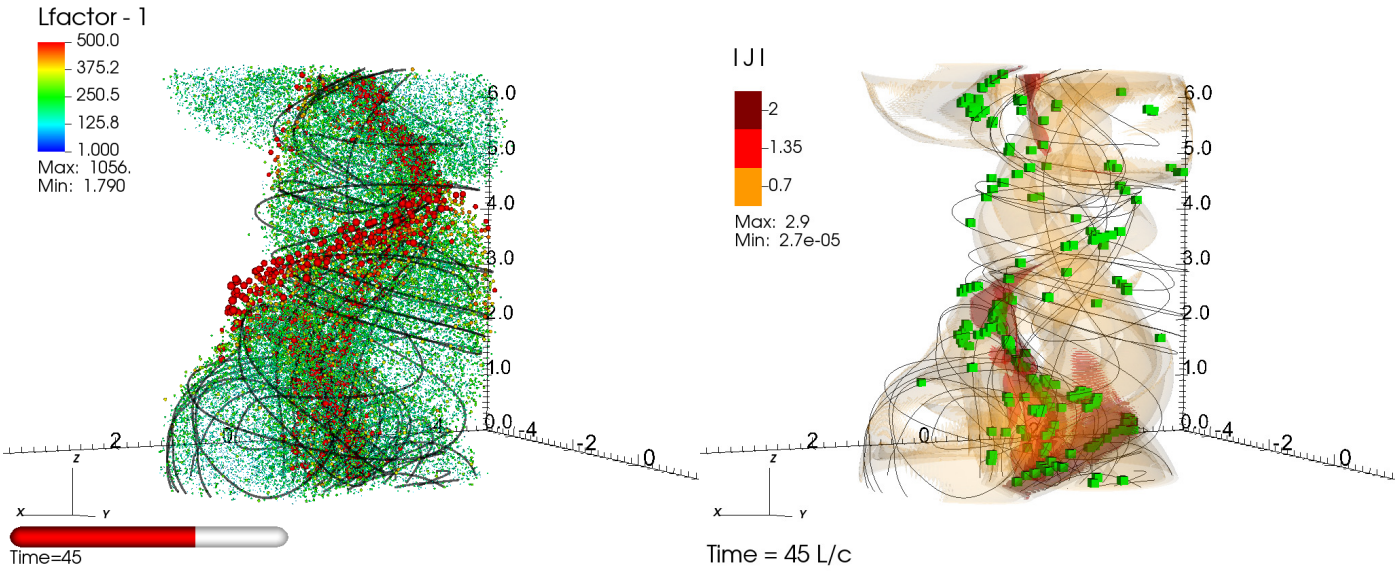

Figura 1. 3D $\sigma \sim 1$ jet evolved with the test particles (MHD-PIC mode) at $t = 45$ L/c. The black lines represent the magnetic field. Left panel: The circles represents the 50,000 particle distribution, the color and size of the circles indicate the value of their kinetic energy normalized by the rest mass energy ($\gamma_p - 1$). Right panel: The orange color represents iso-surfaces of half of the maximum of the current density intensity $|J|$, and the green squares correspond to the positions of the fastest magnetic reconnection events, with reconnection rate ≥ 0.05. See text for more details.

Ackermann et al. 2016; Britto et al. 2016; Aartsen et al. 2018), investigated particle acceleration in a 3D relativistic magnetically dominated jet subject to current driven kink instability (CDKI), by means of relativistic MHD simulations (using the RAISHIN code; Mizuno et al. 2012; Singh et al. 2016). The instability drives turbulence and fast magnetic reconnection in the jet flow. Its growth and saturation causes the excitation of large amplitude wiggles along the jet and the disruption of the initial helical magnetic field configuration, leading to the formation of turbulence and several sites of fast reconnection. The turbulence developed follows approximately a Kolmogorov spectrum (KGM+21). Test protons injected, by GACCEL code in the nearly stationary snapshots of the jet, experience an exponential acceleration in time, predominantly its momentum component parallel to the local field, up to a maximum energy. For a background magnetic field of $B \sim 0.1$ G, this saturation energy is $\sim 10^{16}$ eV, while for $B \sim 10$ G it is $\sim 10^{18}$ eV. There is a clear association of the accelerated particles with the regions of fast reconnection and largest current density. The particles interact with magnetic fluctuations from the small dissipative scales up to the injection scales of the turbulence, which is of the order of the size of the jet diameter. For this reason, the Larmor radius of the particles attaining the saturation energy, which gives the maximum size of the acceleration region, is also of the same order. Beyond the saturation value, the particles suffer further acceleration to energies up to 100 times larger, but at a slower rate, due to drift in the largest scale non-reconnecting fields. The energy spectrum of the accelerated particles develops a high energy tail with a power law index $p \sim$ -1.2 in the beginning of the acceleration, in agreement with earlier works (MGK+21).

In this work, we present a summary of our results of 3D MHD-PIC simulations of $\sigma \sim 1$ relativistic jets (using the PLUTO code; Mignone et al. 2018; Medina-Torrejón et al. 2023), considering in most of the tests the same initial jet setup as in MGK+21 and KGM+21.

2. Results

We performed a 3D MHD-PIC simulation of a relativistic jet using the PLUTO code with non explicit resistivity (for more details see Medina-Torrejón et al. 2023). The computational domain in Cartesian coordinates (x, y, z) has dimensions $10L \times 10L \times 6L$, where L is the length scale unit. We have considered two different initial values of the magnetization parameter $\sigma \sim 1$ and 10. In order to drive turbulence in the jet, we allow for the development of the CDKI by imposing an initial perturbation in the radial velocity profile, as in MGK+21. We perform a dimensionless relativistic jet using the PLUTO code, but to inject the particles with the MHD-PIC mode (particles evolving with the flow) and with the GACCEL code (particles injected in a chosen snapshot of the flow), the trajectories of the test particles require physical values of the relativistic jet to integrate into the plasma fields. We have adopted an initial magnetic field $B \sim 0.1$ G, a density $\rho = 1.67 \times 10^{-24}$ gcm^{-3}, and a physical length scale $L \sim 5.2 \times 10^{-7}$ pc in MHD-PIC mode, and $L = 3.5 \times 10^{-5}$ pc in GACCEL code.

In most of the models, we integrated the trajectories of 1,000–50,000 protons with initial uniform space distribution inside the domain, and initial kinetic energies between $(\gamma_p - 1) \sim 1$ and 200, where γ_p is the particle Lorentz factor, with velocities randomly generated by a Gaussian distribution.

Figure 1 shows the $\sigma \sim 1$ jet evolved with the MHD-PIC mode of the PLUTO code for two snapshots. Initially, a total of 50,000 particles were injected into the system and evolved with the flow. The dynamical evolution of the jet is very similar to the one obtained in MGK+21 and KGM+21 with the RAISHIN MHD code. With the growth of the CDKI, the initial helical magnetic field structure starts to wiggle and then, turbulence develops distorting entirely the field lines and driving fast magnetic reconnection sites, as we see in the right panel. Massive particle acceleration takes place only when turbulence and fast reconnection fully develops in the system, as indicated in the left bottom panel. The correlation of the accelerated particles (represented by the red circles with increasing diameter as

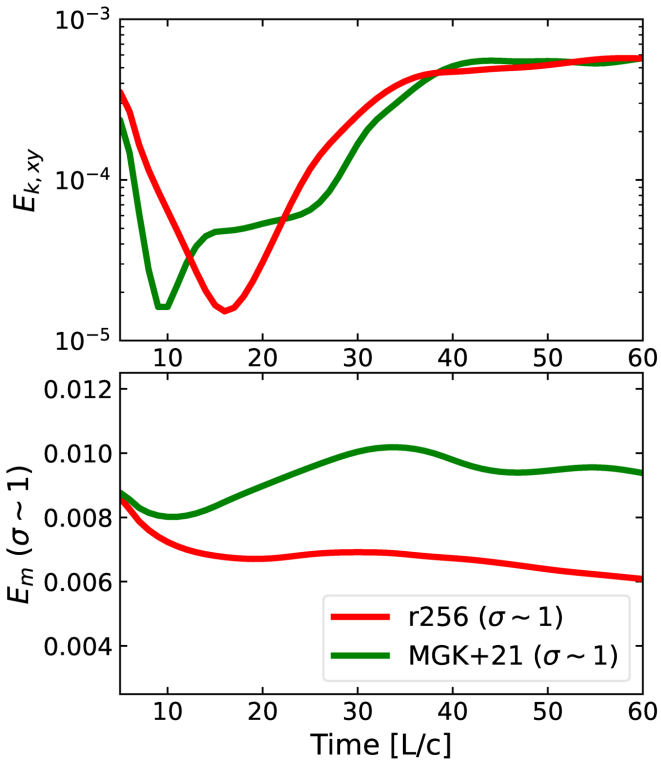

Figura 2. Top: Time evolution of the volume-averaged kinetic energy density transverse to the z-axis within a cylinder of radius $R \leq 3.0L$. Bottom: volume-averaged relativistic electromagnetic energy density for the same models. Red lines corresponds to the results of the jet evolved with PLUTO for the $\sigma \sim 1$, for comparison, also plotted with green lines are the results obtained in MGK+21 for the $\sigma \sim 1$. The kinetic energy is presented in log scale, while E_m is in linear scale.

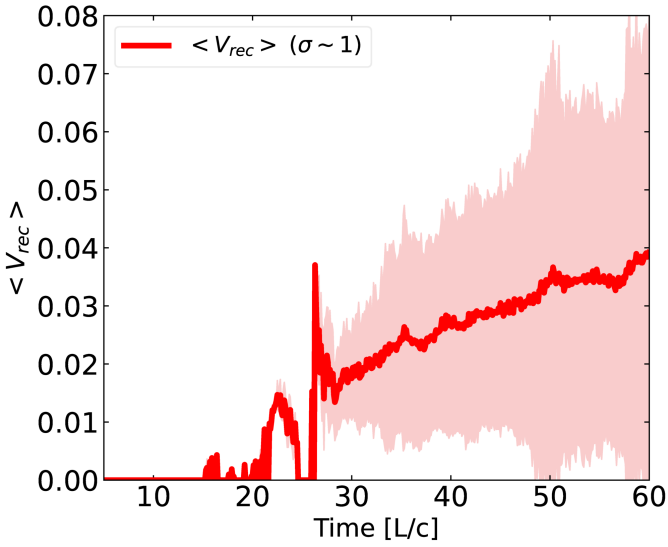

Figura 3. Average reconnection rate evolution, the colored shades correspond to the standard deviations of each model.

the energy increases) with the sites of high current density and fast reconnection (right bottom panel) is evident.

We have used the same algorithm employed in KGM+21 to identify fast magnetic reconnection sites in the turbulent flow and quantify their reconnection velocities (see also, Zhdankin et al. 2013; Kadowaki et al. 2018). The time evolution of the average value of the magnetic reconnection rate, $\langle V_{rec} \rangle$, for all identified sites, in units of the Alfvén velocity, are shown in Figure 3. The evolution of $\langle V_{rec} \rangle$ changes more abruptly after $t \sim 25$, when the CDKI starts to grow exponentially (Figure 2). After that, as the CDKI tends to saturation, the average reconnection rate also attains a value $\langle V_{rec} \rangle \sim 0.03 \pm 0.02$, in agreement with KGM+21.

Figure 2 shows the time evolution of the volume-averaged kinetic energy density transverse to the z-axis (upper panel), and the volume-averaged total relativistic electromagnetic energy density (E_m) (bottom panel) for the $\sigma \sim 1$ jet, as the CDKI grows (see also Mizuno et al. 2012; Singh et al. 2016; Medina-Torrejón et al. 2021). These curves are also compared with those obtained by MGK+21 (and KGM+21) using the RAISHIN code for the same jet model (labeled as MGK+21 in Figure **??**), and with the $\sigma \sim 10$ jet. Note that E_m is presented in the linear scale, while the kinetic energy is in the log scale. The results of both $\sigma \sim 1$ jet models are comparable. As the CDKI develops, E_m is converted into kinetic energy. The initial relaxation of the system to equilibrium leads to a hump in the kinetic and E_m curves. After this relaxation, there is an initial growth of E_m caused by the increasing wiggling distortion of the magnetic field structure in the jet spine due to the initial growth of the CDKI. The kinetic energy, after a slower increase, undergoes an exponential growth.

Top pannel of Figure 4 depicts the kinetic energy growth as a function of time for 1,000 particles injected (with the GACCEL code, with an initial Maxwellian distribution with initial mean kinetic energy $\langle E_p \rangle \sim 10^{-2} m_p c^2$) in the fully turbulent jet simulated with the PLUTO code, at $t = 45$ L/c. As in MGK+21, particles are accelerated exponentially in the magnetic reconnection sites in all scales of the turbulence driven by the CDKI up to $\sim 10^7 mc^2$, which corresponds to a Larmor radius comparable to the diameter of the jet and the size of the largest turbulent magnetic structures (see the plot in the inset). The parallel component of the velocity is predominantly accelerated in the exponential regime, as expected in a Fermi-type process, while in the drift regime, it is the perpendicular component that prevails (see MGK+21 and Medina-Torrejón et al. (2023) for more details).

Bottom panel of Figure 4 shows the first stages of the kinetic energy evolution of the particles evolving together with the background jet as obtained with the present model (i.e., employing the MHD-PIC mode). In the very beginning, while the CDKI is still developing, particles only suffer drift in the background magnetic fields. After $t \sim 30$ L/c, which coincides with the nonlinear growth and saturation of the CDKI leading to fully developed turbulence in the jet (Figures 2), the particles in the bottom panel of the Figure 4 start exponential acceleration, as in the top pannel of Figure 4. The entire dynamical time of the system evolution is of only 60 L/c. For the particles, the physical time elapsed is only $\sim 60L/c \sim 1$ hr, which is much smaller than the several hundred hours that particles can accelerate in the nearly steady state jet snapshot (top pannel of Figure 4) where they can re-enter the system several times through the periodic boundaries of the jet in the z direction until they reach the saturation energy (see also MGK+21). This explains why particles do not achieve the maximum possible energy by acceleration in the largest turbulent magnetic reconnection structures of the order of the jet diameter ($\sim 4L$), as we see in the inset in the figure, which depicts the particles Larmor radius distribution. For this value of the Larmor radius ($R_{max} \sim 4L$), the particles would achieve an energy $E_{sat} \sim e\,B\,R_{max} \sim 200,000\ m_p c^2$ in the $\sigma \sim 1$ jet, if the jet were allowed to evolve for a dynamical time about

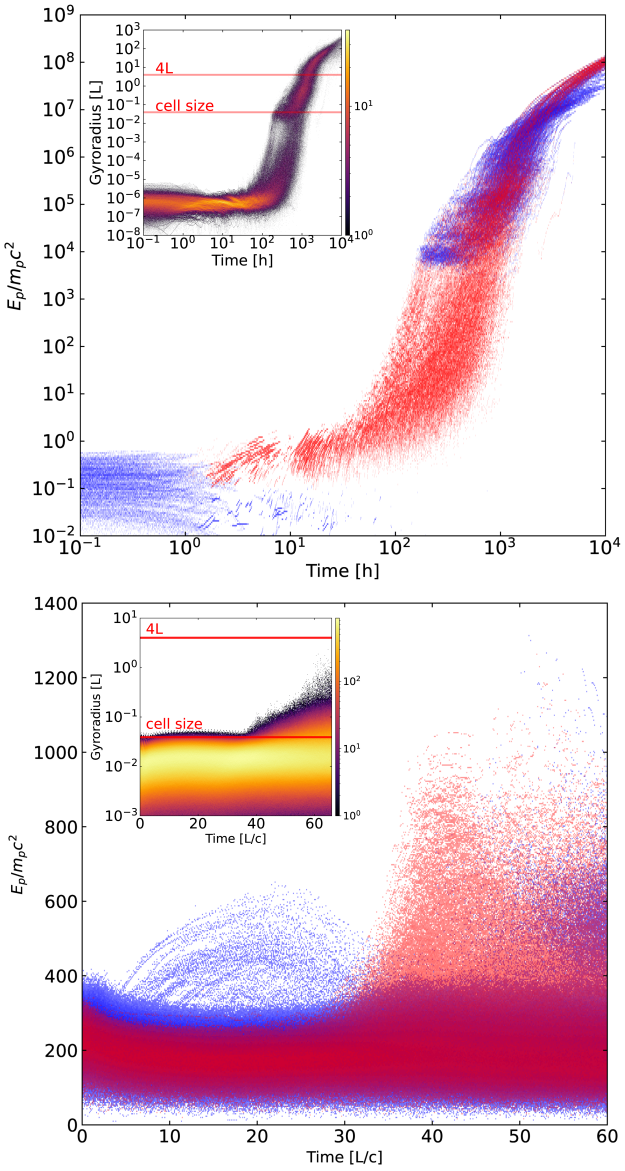

Figura 4. Kinetic energy evolution, normalized by the proton rest mass energy. Top panel: 1,000 particles injected into the fully turbulent snapshot $t = 45$ L/c of the $\sigma \sim 1$ jet with an initial Maxwellian distribution with initial kinetic energy $\langle E_p \rangle \sim 10^{-2} m_p c^2$, the particle acceleration time is given in hours and the adopted physical size for L is the same as in MGK+21 for comparison, $L = 3.5 \times 10^{-5}$ pc. Bottom panel: 50,000 particles evolved in the MHD-PIC simulation for the $\sigma \sim 1$ jet, injected with energy $\langle E_p \rangle \sim 1 - 200 m_p c^2$, and $L \sim 5.2 \times 10^{-7}$ pc. The colors indicate which velocity component is being accelerated (red or blue for the parallel or perpendicular component to the local magnetic field, respectively). The insets in the upper left corner show the time evolution of the particles gyroradius. The color bars indicate the number of particles. The horizontal grey stripe is bounded on the upper part by the jet diameter ($4L$) and on lower part by the cell size of the simulated background jet.

one hundred times larger (where $R_{max} \sim 4L = 2.1 \times 10^{-6}$ pc, and $B \sim 0.1$ G, considering the physical units employed in the MHD-PIC simulations). Nonetheless, the results in these early stages of particle acceleration, follow the same trend depicted in top pannel of Figure 4, indicating that particles are accelerated exponentially by magnetic reconnection in the turbulent flow, from the small resistive scales up to the large scales of the turbulence in the ideal electric field of the magnetic reconnecting structures. These results also indicate that the time evolution of the background magnetic fields does not influence the acceleration of the particles since they enter the exponential regime of acceleration in the same jet dynamical times in which turbulence becomes fully developed, as obtained in the MHD simulations with test particles of top pannel of Figure 4.

3. Conclusões

The results found in this work have important implications for particle acceleration and the associated non-thermal emission in relativistic jets, specially in their magnetically dominated regions. These results (and those produced in earlier MHD works with test particles; e.g. Kowal et al. 2012; del Valle et al. 2016; Medina-Torrejón et al. 2021) are in contrast with recent studies based on 3D PIC simulations that suggest that acceleration by reconnection would be dominant only in the very early stages of particle energizing (e.g., Comisso and Sironi 2019; Sironi et al. 2021; Sironi 2022; Comisso and Sironi 2022).

Protons with these energies achieved by our results could explain the observed very high energy emissions, as well as the production of neutrinos, from interactions with ambient photons and density fields in relativistic jets (Aartsen et al. 2018).

Agradecimentos. The authors acknowledge very useful discussions with L. Kadowaki. TEMT acknowledge support from the Brazilian Funding Agency FAPESP (grant 2023/08554-7), EMdGDP acknowledge support from FAPESP (grant 13/10559-5), EMdGDP also acknowledges support from CNPq (grant 308643/2017-8), and G.K. from FAPESP (grants 2013/10559-5, 2019/03301-8, and 2021/06502-4). The simulations presented in this work were performed in the cluster of the Group of Plasmas and High-Energy Astrophysics (GAPAE), acquired with support from FAPESP (grant 2013/10559-5), and the computing facilities of the Laboratory of Astroinformatics (IAG/USP, NAT/Unicsul), whose purchase was also made possible by FAPESP (grant 2009/54006-4) and the INCT-A.

Referências

Aartsen, M., Ackermann, M., Adams, J., Aguilar, J. A., Ahlers, M., and Ahrens (2018). Neutrino emission from the direction of the blazar txs 0506+056 prior to the icecube-170922a alert. *Science*, 361(6398):147–151.

Ackermann, M., Anantua, R., Asano, K., and et al. (2016). Minute-timescale >100 MeV γ-Ray Variability during the Giant Outburst of Quasar 3C 279 Observed by Fermi-LAT in 2015 June. *ApJ*, 824(2):L20.

Aharonian, F., Akhperjanian, A. G., Bazer-Bachi, A. R., and et al. (2007). An Exceptional Very High Energy Gamma-Ray Flare of PKS 2155-304. *ApJ*, 664(2):L71–L74.

Ball, D., Sironi, L., and Özel, F. (2018). Electron and Proton Acceleration in Trans-relativistic Magnetic Reconnection: Dependence on Plasma Beta and Magnetization. *ApJ*, 862(1):80.

Bell, A. R., Araudo, A. T., Matthews, J. H., and Blundell, K. M. (2018). Cosmic-ray acceleration by relativistic shocks: limits and estimates. *MNRAS*, 473(2):2364–2371.

Beresnyak, A. and Li, H. (2016). First-Order Particle Acceleration in Magnetically-driven Flows. *ApJ*, 819(2):90.

Britto, R. J., Bottacini, E., Lott, B., Razzaque, S., and Buson, S. (2016). Fermi-LAT Observations of the 2014 May-July Outburst from 3C 454.3. *ApJ*, 830(2):162.

Cerutti, B., Werner, G. R., Uzdensky, D. A., and Begelman, M. C. (2013). Simulations of Particle Acceleration beyond the Classical Synchrotron Burnoff Limit in Magnetic Reconnection: An Explanation of the Crab Flares. *ApJ*, 770(2):147.

Christie, I. M., Petropoulou, M., Sironi, L., and Giannios, D. (2019). Radiative signatures of plasmoid-dominated reconnection in blazar jets. *MNRAS*, 482(1):65–82.

Comisso, L. and Sironi, L. (2019). The Interplay of Magnetically Dominated Turbulence and Magnetic Reconnection in Producing Nonthermal Particles. *ApJ*, 886(2):122.

Comisso, L. and Sironi, L. (2022). Ion and Electron Acceleration in Fully Kinetic Plasma Turbulence. *ApJ*, 936(2):L27.

de Gouveia Dal Pino, E. M. and Kowal, G. (2015). *Particle Acceleration by Magnetic Reconnection*, volume 407 of *Astrophysics and Space Science Library*, page 373. Springer Berlin Heidelberg.

de Gouveia Dal Pino, E. M. and Lazarian, A. (2005). Production of the large scale superluminal ejections of the microquasar GRS 1915+105 by violent magnetic reconnection. *A&A*, 441(3):845–853.

de Gouveia Dal Pino, E. M., Piovezan, P. P., and Kadowaki, L. H. S. (2010). *The role of magnetic reconnection on jet/accretion disk systems*. *A&A*, 518:5.

del Valle, M. V., de Gouveia Dal Pino, E. M., and Kowal, G. (2016). Properties of the first-order Fermi acceleration in fast magnetic reconnection driven by turbulence in collisional magnetohydrodynamical flows. *MNRAS*, 463:4331–4343.

Drake, J. F., Swisdak, M., Che, H., and Shay, M. A. (2006). Electron acceleration from contracting magnetic islands during reconnection. *Nature*, 443(7111):553–556.

Giannios, D., Uzdensky, D. A., and Begelman, M. C. (2009). Fast TeV variability in blazars: jets in a jet. *MNRAS*, 395(1):L29–L33.

Guo, F., Li, X., Daughton, W., Kilian, P., Li, H., Liu, Y.-H., Yan, W., and Ma, D. (2019). Determining the Dominant Acceleration Mechanism during Relativistic Magnetic Reconnection in Large-scale Systems. *ApJ*, 879(2):L23.

Guo, F., Liu, Y.-H., Daughton, W., and Li, H. (2015). Particle Acceleration and Plasma Dynamics during Magnetic Reconnection in the Magnetically Dominated Regime. *ApJ*, 806(2):167.

Guo, F., Liu, Y.-H., Li, X., Li, H., Daughton, W., and Kilian, P. (2020). Recent progress on particle acceleration and reconnection physics during magnetic reconnection in the magnetically-dominated relativistic regime. *Physics of Plasmas*, 27(8):080501.

Hoshino, M. and Lyubarsky, Y. (2012). Relativistic Reconnection and Particle Acceleration. *Space Sci. Rev.*, 173(1-4):521–533.

Hovatta, T. and Lindfors, E. (2019). Relativistic Jets of Blazars. *New A Rev.*, 87:101541.

Kadowaki, L. H. S., de Gouveia Dal Pino, E. M., Medina-Torrejón, T. E., Mizuno, Y., and Kushwaha, P. (2021). Fast Magnetic Reconnection Structures in Poynting Flux-dominated Jets. *ApJ*, 912(2):109.

Kadowaki, L. H. S., de Gouveia Dal Pino, E. M., and Singh, C. B. (2015). The Role of Fast Magnetic Reconnection on the Radio and Gamma-ray Emission from the Nuclear Regions of Microquasars and Low Luminosity AGNs. *ApJ*, 802:113.

Kadowaki, L. H. S., de Gouveia Dal Pino, E. M., and Stone, J. M. (2018). MHD Instabilities in Accretion Disks and Their Implications in Driving Fast Magnetic Reconnection. *ApJ*, 864(1):52.

Kilian, P., Li, X., Guo, F., and Li, H. (2020). Exploring the Acceleration Mechanisms for Particle Injection and Power-law Formation during Transrelativistic Magnetic Reconnection. *ApJ*, 899(2):151.

Kowal, G., de Gouveia Dal Pino, E. M., and Lazarian, A. (2011). Magnetohydrodynamic Simulations of Reconnection and Particle Acceleration: Three-dimensional Effects. *ApJ*, 735(2):102.

Kowal, G., de Gouveia Dal Pino, E. M., and Lazarian, A. (2012). Particle Acceleration in Turbulence and Weakly Stochastic Reconnection. *Phys. Rev. Lett.*, 108(24):241102.

Matthews, J., Bell, A., and Blundell, K. (2020). Particle acceleration in astrophysical jets. *arXiv e-prints*, page arXiv:2003.06587.

McKinney, J. C. and Uzdensky, D. A. (2012). A reconnection switch to trigger gamma-ray burst jet dissipation. *MNRAS*, 419(1):573–607.

Medina-Torrejón, T. E., de Gouveia Dal Pino, E. M., Kadowaki, L. H. S., Kowal, G., Singh, C. B., and Mizuno, Y. (2021). Particle Acceleration by Relativistic Magnetic Reconnection Driven by Kink Instability Turbulence in Poynting Flux-Dominated Jets. *ApJ*, 908(2):193.

Medina-Torrejón, T. E., de Gouveia Dal Pino, E. M., and Kowal, G. (2023). Particle Acceleration by Magnetic Reconnection in Relativistic Jets: The Transition from Small to Large Scales. *ApJ*, 952(2):168.

Mehlhaff, J. M., Werner, G. R., Uzdensky, D. A., and Begelman, M. C. (2020). Kinetic beaming in radiative relativistic magnetic reconnection: a mechanism for rapid gamma-ray flares in jets. *MNRAS*, 498(1):799–820.

Mignone, A., Bodo, G., Vaidya, B., and Mattia, G. (2018). A Particle Module for the PLUTO Code. I. An Implementation of the MHD-PIC Equations. *ApJ*, 859(1):13.

Mizuno, Y., Gómez, J. L., Nishikawa, K.-I., Meli, A., Hardee, P. E., and Rezzolla, L. (2015). Recollimation Shocks in Magnetized Relativistic Jets. *ApJ*, 809(1):38.

Mizuno, Y., Lyubarsky, Y., Nishikawa, K.-I., and Hardee, P. E. (2012). Three-dimensional Relativistic Magnetohydrodynamic Simulations of Current-driven Instability. III. Rotating Relativistic Jets. *ApJ*, 757(1):16.

Singh, C. B., Mizuno, Y., and de Gouveia Dal Pino, E. M. (2016). Spatial Growth of Current-driven Instability in Relativistic Rotating Jets and the Search for Magnetic Reconnection. *ApJ*, 824:48.

Sironi, L. (2022). Nonideal Fields Solve the Injection Problem in Relativistic Reconnection. *Phys. Rev. Lett.*, 128(14):145102.

Sironi, L., Petropoulou, M., and Giannios, D. (2015). Relativistic jets shine through shocks or magnetic reconnection? *MNRAS*, 450(1):183–191.

Sironi, L., Rowan, M. E., and Narayan, R. (2021). Reconnection-driven Particle Acceleration in Relativistic Shear Flows. *ApJ*, 907(2):L44.

Sironi, L. and Spitkovsky, A. (2014). Relativistic Reconnection: An Efficient Source of Non-thermal Particles. *ApJ*, 783(1):L21.

Sironi, L., Spitkovsky, A., and Arons, J. (2013). The Maximum Energy of Accelerated Particles in Relativistic Collisionless Shocks. *ApJ*, 771(1):54.

Zenitani, S. and Hoshino, M. (2001). The Generation of Nonthermal Particles in the Relativistic Magnetic Reconnection of Pair Plasmas. *Apjl*, 562:L63–L66.

Zenitani, S. and Hoshino, M. (2007). Particle Acceleration and Magnetic Dissipation in Relativistic Current Sheet of Pair Plasmas. *ApJ*, 670(1):702–726.

Zhang, B. and Yan, H. (2011). The Internal-collision-induced Magnetic Reconnection and Turbulence (ICMART) Model of Gamma-ray Bursts. *ApJ*, 726:90.

Zhang, H., Li, X., Guo, F., and Giannios, D. (2018). Large-amplitude Blazar Polarization Angle Swing as a Signature of Magnetic Reconnection. *ApJ*, 862(2):L25.

Zhang, H., Sironi, L., Giannios, D., and Petropoulou, M. (2023). The Origin of Power-law Spectra in Relativistic Magnetic Reconnection. *ApJ*, 956(2):L36.

Zhdankin, V., Uzdensky, D. A., Perez, J. C., and Boldyrev, S. (2013). Statistical Analysis of Current Sheets in Three-dimensional Magnetohydrodynamic Turbulence. *ApJ*, 771(2):124.